Influence of selected alloying elements on the stability of magnesium dihydride for hydrogen storage applications: A first-principles investigation

Y. Song,[1,*] Z. X. Guo,[1] and R. Yang[2]
[1]*Department of Materials, Queen Mary, University of London, Mile End Road, London E1 4NS, United Kingdom*
[2]*Institute of Metal Research, Chinese Academy of Sciences, 72 Wenhua Road, Shenyang 110016, China*
(Received 25 March 2003; revised manuscript received 12 December 2003; published 25 March 2004)

MgH_2 is a promising compound for hydrogen storage. Its relatively high stability has been the main obstacle for practical applications. Here, first-principles calculations of MgH_2 and MgH_2-X (X=Al, Ti, Fe, Ni, Cu, or Nb) were carried out to investigate the influences of selected alloying elements on the stability of the magnesium hydride. The full-potential linearized augmented plane-wave method within the generalized gradient approximation was used in the present study. The influence of alloying elements on the stability of magnesium dihydride was investigated through calculations of the total energy of the considered systems. It was shown that the alloying elements considered here decrease the heat of formation of $(Mg,X)H_2$—i.e., destabilizing the hydride—with decreasing order of effect from Cu, Ni, Al, Nb, and Fe to Ti. The destabilization of the magnesium hydride by the alloying elements was due to a weakened bonding between magnesium and hydrogen atoms. Hence, the dehydrogenation properties of MgH_2 are expected to be improved to a different extent by the addition of alloying elements.

DOI: 10.1103/PhysRevB.69.094205 PACS number(s): 61.50.Ah, 61.66.Dk

I. INTRODUCTION

A desirable material for ''on-board'' vehicular storage of hydrogen should possess a high hydrogen density and rapid discharge kinetics at a sufficiently low temperature to utilize exhaust-gas waste heat. Magnesium alloys exhibit some outstanding features for such applications. The hydrogen storage capacity of pure MgH_2 is 7.6 wt %, with a formation enthalpy of -76 kJ/mol H_2. However, its slow hydriding and dehydriding kinetics and high dissociation temperature currently limit its practical applications for hydrogen storage.[1] The main objective of many current studies has been to reduce the high Mg-H binding energy by alloying additions, so as to reduce the sorption temperature.

Numerous studies have been carried out in order to identify a suitable alloy that absorbs hydrogen close to room temperature and desorbs hydrogen at a temperature low enough to use the waste heat of exhaust gas.[2–4] It has been reported experimentally that mixing magnesium with catalytic transition elements, such as Ti, V, Fe, Co, and Ni, effectively improves the hydriding and dehydriding kinetics of magnesium at high temperatures (>573 K).[5,6] Ti and V, when mixed with the magnesium hydride by ball milling, are better catalysts than Ni for magnesium hydrides.[6] Although Ni is commonly used for hydrogen absorption in Mg and its alloys, it is not as good a catalyst as Ti and V. This has been attributed to the effect of oxygen. Titanium and vanadium have very strong affinities to oxygen, and their oxides cannot be reduced by hydrogen under normal conditions, while NiO can be readily reduced by hydrogen to form nickel clusters on the surfaces.[7] This is the reason that Ni has better catalytic effects than Ti and V in conventional Mg-based alloys. Mechanical milling of MgH_2 with Ti or V leads to titanium or vanadium hydrides, which could protect Ti or V from oxidation, and therefore the catalytic effect towards hydrogen is preserved.[6]

It is desirable to understand the intrinsic mechanisms of alloying effects on the properties of the magnesium hydride. In the present study, we intend to investigate the influences of selected alloying elements on the hydrogen storage properties of magnesium hydride, particularly the stability of the compound. To this end, we have calculated the total energy and, then, the heat of the formation of the MgH_2 and $(Mg,X)H_2$ (X=Al, Ti, Fe, Ni, Cu, or Nb) with the full-potential linearized augmented plane-wave (FP-LAPW) method. As a result of the calculation, it is noted that the calculated heat of formation of MgH_2 reproduces the experimental value. From a detailed analysis of the calculated heat of formation and the electronic structure of the considered systems, it is noted that the bonding between magnesium and hydrogen atoms was weakened by the additional elements.

II. METHOD OF CALCULATION

The thermodynamic aspects of hydride formation from gaseous hydrogen are described by pressure-composition isotherms. The host metal initially dissolves some hydrogen to form a solid solution (α phase). As the hydrogen pressure together with the concentration of H in the metal is increased, interactions between hydrogen atoms become locally important and then lead to the formation of the hydride (β) phase. While the two phases coexist, the pressure-composition isotherms show a flat plateau, the length of which determines how much H_2 can be stored reversibly with small pressure variations. The plateau or equilibrium pressure depends strongly on temperature and is related to the changes of enthalpy (ΔH) and entropy (ΔS).

As the entropy change corresponds mostly to the change from molecular hydrogen gas to dissolved hydrogen, it is roughly 130 $JK^{-1}mol^{-1}$ for all metal-hydrogen systems under consideration. The enthalpy term ΔH, the heat of forma-

tion of a hydride, characterizes the stability of the metal-hydrogen bond. There are many models to estimate the heat of formation of a hydride.[8–11] One of the most successful is that of Bouten and Miedema,[8] based on Miedema's original approach to the heat of formation of two transition metals,[12] and was generalized to ternary metal hydrides AB_nH_{2m} using the rule of reversed stability, where the transition metal A is assumed to have a stronger affinity to hydrogen than the transition metal B and, as a result, hydrogen atoms are attracted to the A atoms in the AB_n compounds and ''shield'' the A atoms from the surrounding B atoms.[13] By means of this approach the heat of formation of AB_nH_{2m} hydrides is approximately given by

$$\Delta H(AB_nH_{2m}) = \Delta H(AH_m) + \Delta H(B_nH_m) - \Delta H(AB_n). \quad (1)$$

The breaking of the A-B bonds is accounted for by the last term in Eq. (1). Generally speaking, the first term on the right-hand side of Eq. (1) is negative and has the largest absolute value, whereas the second term is relatively small and may be positive. Therefore, the sum of the first and second terms is almost a constant for any alloy that has the same hydrogen-absorbing metal. This means that if the last term in Eq. (1) becomes more negative—i.e., the alloy AB_n is more stable—the left-hand side of Eq. (1) is more positive—i.e., the hydride is less stable. Therefore, the hydride stability decreases when the stability of the alloy AB_n increases. This model can be applied to the case that A and B form a compound only. In some cases—for example, the MgH_2-Ti system—there exists no compound between Mg and Ti. Then Eq. (1) cannot be used to estimate the heat of formation of such systems.

In principle, theoretical evaluation of the hydride stability can be made directly from the total energy of the alloys involved in the hydrogenation reaction. There are some *ab initio* calculations of the heat of formation for the $LaNi_5$,[14–16] Mg_2NiH_4,[17] and K_2PtCl_6-type intermetallic hydrides,[18] CsCl-type titanium compounds,[19] and transition metal dihydrides.[20] No similar studies have been carried out on the MgH_2 system.

In the present work we employ *ab initio* calculations based on the FP-LAPW method to study the energies and evolution of the electronic charge density of the magnesium hydrides with and without alloying addition. The full-potential linearized augmented plane-wave code WIEN2K (Ref. 21) was used in the present work. In brief, this is an implementation of the density functional theory with different possible approximations for the exchange and correlation potential. The Kohn-Sham equations are solved using a basis of linearized augmented plane waves.[22] The Perdew-Burke-Ernzerhof[23] generalized gradient approximation (GGA) exchange and correlation potential was used in the calculations. A muffin-tin radius was chosen as 1.8 bohr for both Mg and alloying atoms and 1.5 bohr for the hydrogen atom. The self-consistency procedure was performed with 1000 **k** points in the irreducible part of the Brillouin zone. The total energy was computed according to Weinert *et al.*[24] In all calculations, self-consistency was achieved with a tolerance in the total energy of 0.1 mRy.

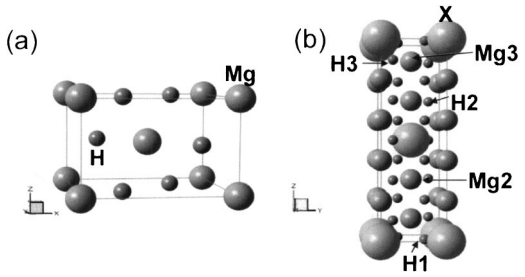

FIG. 1. Schematic of atomic cells used in the calculation: (a) unit cell of MgH_2 and (b) supercell, where the nonequivalent atomic positions are denoted by 1, 2, and 3.

III. RESULTS

A. Stability

MgH_2 has a tetragonal symmetry ($P4_2/mnm$, group No. 136). The Mg atom occupies the $2a(0,0,0)$ site and the H atom the $4f(0.304,0.304,0)$ site, Fig. 1(a). The lattice parameters are $a=0.4501$ nm and $c=0.301$ nm.[25] In this study we employed a supercell 5 times the size of the unit cell in the c axis, Fig. 1(b). Due to the symmetry requirement, there are three nonequivalent sites for magnesium and hydrogen atoms in the supercell, as detailed in Table I. To investigate the influence of the alloying elements on the stability and on the total energy and the electronic structure of the hydrides, two Mg atoms in the supercells were replaced by alloying atoms.

The influence of alloying elements on the stability of the magnesium hydride was studied by calculation of the total energy of the alloyed magnesium dihydride. To consider the relaxation induced by the alloying elements, geometric optimizations of the magnesium dihydride with and without alloying elements were performed by first varying the supercell volume while fixing the c/a ratio as a constant. The variation of the total energy against the lattice parameter a is

TABLE I. Structure of the supercell used in the present calculation.[a]

Atom	x	y	z	Number of atoms
Mg1 (X)	0	0	0	2
Mg2	0	0	0.2	4
Mg3	0	0	0.6	4
H1	0.304	0.304	0	4
H2	0.196	0.804	0.1	8
H3	0.304	0.304	0.2	8

[a]The space group of the supercell is $P4_2/mnm$ (No. 136) with lattice parameters of $a=0.4501$ nm, $c'=5c=1.503$ nm. The nonequivalent atoms are denoted by the numbers 1, 2, and 3. x, y, and z are atomic coordinates in terms of lattice vectors a, b, and c, respectively. The symbol X denotes that the Mg1 atom will be replaced by an alloying atom X in the MgH_2-X systems.

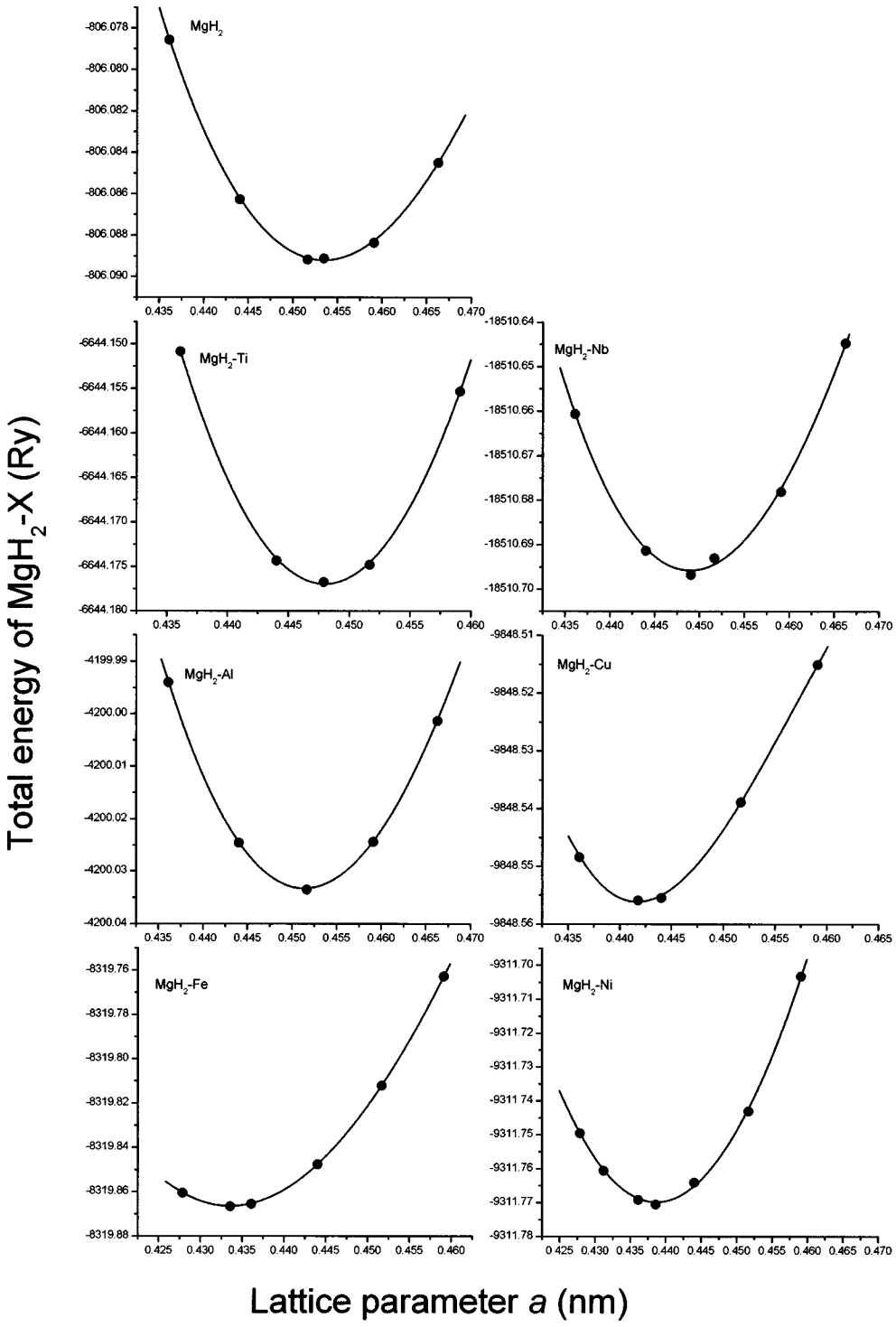

FIG. 2. Total energy curves against the lattice parameter a with a constant ratio of c_0/a_0 of the MgH_2-X systems.

plotted in Fig. 2, where the data are fitted to a third-order polynomial. Accordingly, the lattice parameters were estimated from the minimized total energy points of the considered systems. The estimated lattice parameters a and c of MgH_2 are 0.4535 nm and 0.3033 nm, respectively, which are very close to the experimental values of $a=0.4501$ nm and $c=0.301$ nm.[25] Then the full geometric relaxation was carried out for the alloyed systems using the lattice parameters estimated from Fig. 2 as the starting point with 100 **k** points for computational efficiency. The dependence of the accuracy of the calculated total energy with the **k** points was estimated. For example, the total energy of MgH_2-Nb is $-18\,510.696\,526$ (Ry) for the 100 **k** points and $-18\,510.698\,842$ (Ry) for the 1000 **k** points. The relaxation was performed by changing the lattice parameters a and c independently. Therefore the lattice parameters a and c of the considered MgH_2-X systems were reestimated from the minimum area of the energy surface via a and c. The values

TABLE II. Lattice parameters a and c in nm, relative change of the atomic coordinates $\Delta z = z - z_0$, $\Delta x = x - x_0$, and the total energies of the MgH_2 and $MgH_2 - X$ systems after the full geometry optimization of the supercell.

	Lattice parameters						
	a (nm)	c (nm)	Δz(Mg2)	Δz(Mg3)	Δx(H2)	Δx(H3)	Total energy E_{tot} (Ry)
MgH_2	0.4535	0.3033					−806.089126 (unit cell)
Al	0.4515	0.3020	0.0001	0.0001	0.0006	0.0112	−4200.040855
Ti	0.4475	0.2994	0.0001	0.0002	0.0008	0.0006	−6644.177974
Fe	0.4333	0.2850	0.0000	−0.0001	0.0007	0.0231	−8319.915554
Ni	0.4379	0.2993	0.0000	−0.0001	0.0006	0.0124	−9311.834185
Cu	0.4420	0.3171	0.0000	0.0006	0.0008	0.0008	−9848.619694
Nb	0.4487	0.3049	0.0002	0.0000	0.0004	0.0007	−18510.698842

of the lattice parameters a and c are listed in Table II. Analysis of the forces shows that (a) the force on the alloying atom is $\mathbf{F}(X) = 0$, (b) the forces on the Mg2, Mg3, and H1 atoms are zero in the x and y directions, but nonzero in the z direction, and (c) the forces on the H2 and H3 atoms are zero in the z direction, but nonzero in the x and y directions. Using these lattice parameters, internal relaxation of the atoms within the supercell was carried out for the alloyed systems. As required by group symmetry, the atoms X and H1 were fixed during the relaxation [Fig. 1(b)]. Then the internal relaxation was performed in two steps. First, the Mg2 and Mg3 atoms were relaxed independently along the z direction, while the H2 and H3 atoms were kept at their initial positions. The variation of the atomic coordinates of the Mg2 or Mg3 atoms was defined as $\Delta z(\mathrm{Mg2/Mg3}) = z - z_0$, where z_0 is the initial atomic coordinate of the Mg2 or Mg3 atom (Table I). The energy surface as a function of the Δz(Mg2) and Δz(Mg3) was constructed and the final values of Δz(Mg2) and Δz(Mg3) were estimated from the minimum area of the energy surface and are listed in Table II. The changes of the position of the Mg2 and Mg3 atoms in the z direction are very small due to the addition of the alloying elements, owing to the fact that the Mg2 and Mg3 atoms are the second nearest-neighbor atoms, resulting in a small energy difference between the relaxed and unrelaxed positions (within 0.3 mRy for the considered alloyed systems). Second, the Mg2 and Mg3 atoms were fixed at their new positions, and the H2 and H3 atoms were relaxed along the x direction independently, with the change of $\Delta x = x - x_0$, where x_0 is the initial atomic coordinate of the two atoms in the supercell (Table I). The H2 and H3 atoms were maintained in $8j$ symmetry ($x = y$) in the supercell during the relaxation. Again, the final values of the Δx(H2) and Δx(H3) were estimated from the total energy surface and are listed in Table II. The value of the Δx(H2) is smaller than that of the Δx(H3). This is consistent with the fact that the H3 atom is the nearest neighbor of the alloying atom in the present supercell (Fig. 1).

In brief, from the relaxation study, it is noted that the alloying elements mainly influence the position of the matrix atoms in their vicinity: i.e., only the positions of the nearest-neighbor H3 atoms were significantly changed. The influence of alloying elements on the position of the H3 atoms increases in the order of Ti, Nb, Cu, Al, and Ni to Fe. Partial densities of states show that the bonding between the d electrons and H3 s electrons is much stronger in the MgH_2-Fe and the MgH_2-Ni than that in the MgH_2-Ti and MgH_2-Nb systems (Figs. 4–6). This is the reason why the influence of the Fe and Ni atoms on the position of the H3 atoms is much stronger than that of the Ti and Nb atoms.

Using these structural parameters, we recalculated the electronic structure and total energy of the alloyed magnesium hydrides with 1000 **k** points. The resulting total energies are also listed in Table II. The lattice parameters in Table II show that the unit cell volume of MgH_2 was reduced by the alloying elements considered in the present work. The level of the reduction of the unit cell volume increases from Cu, Al, Nb, Ti, and Ni to Fe. The variation of the unit cell volume influences the hydrogen storage properties of magnesium dihydrides as will be discussed below.

The heats of formation of hydrogen in solution and in the hydride were calculated by subtracting the total energies of the host alloy and the absorbed hydrogen molecule from that of the final state:

$$\Delta H_{\mathrm{MgH2}} = E_{\mathrm{tot}}(\mathrm{MgH_2}) - E_{\mathrm{tot}}(\mathrm{Mg}) - E_{\mathrm{tot}}(\mathrm{H_2}). \qquad (2)$$

The total energy of the hydrogen molecule was calculated using the same code as used previously with an equilibrium bond length of 0.74 nm. The result is −2.324 803 Ry, very close to the value of −2.320 Ry obtained by using the von Barth–Hedin exchange-correlation potential.[14] The resulting heat of formation of MgH_2 is $-71.149\ \mathrm{kJ/mol\,H_2}$, which is very close to $-76.15 \pm 9.2\ \mathrm{kJ/mol\,H_2}$ measured experimentally.[26]

In order to investigate the influence of alloying elements on the stability of the magnesium dihydride, a parameter ΔE_r was introduced to estimate the relative stability of the alloyed magnesium dihydrides compared with that of MgH_2. The definition of ΔE_r is

$$\Delta E_r = E_{\mathrm{tot}}(\mathrm{Mg_8}X_2\mathrm{H_{20}}) - 10E_{\mathrm{tot}}(\mathrm{MgH_2}) - 2[E^e_{\mathrm{tot}}(X) - E^e_{\mathrm{tot}}(\mathrm{Mg})], \qquad (3)$$

TABLE III. Total energy of pure metal considered in the present study, E^e_{tot}, and the parameter ΔE_r defined by Eq. (3), which describes the relative stability of alloyed MgH_2-X compared to MgH_2.

	E^e_{tot} (Ry/atom)	ΔE_r (kJ/molH_2)
Mg	−400.665547	0
Al	−485.639253	46.21
Ti	−1707.618998	22.91
Fe	−2545.527570	33.34
Ni	−3041.616215	67.88
Cu	−3310.016085	69.12
Nb	−7640.927552	35.53

where the first two terms on the right-hand side are the total energy of the MgH_2-X with the current supercell and that of MgH_2, respectively. $E^e_{\text{tot}}(X)$ denotes the total energy of the element X and was calculated using the same code as for the MgH_2-X. The values of $E^e_{\text{tot}}(X)$ and ΔE_r are listed in Table III. The data in Table III show that the stability of the magnesium dihydride was reduced by the alloying elements: for example, an increase in energy of 22.91 kJ/mol H_2 due to alloying with titanium is noted. The amount of reduction increases in the order of Ti, Fe, Nb, Al, and Ni to Cu. It is noted that the ΔE_r values for the MgH_2-Ni and MgH_2-Cu systems are very close to the absolute value of the heat of formation of MgH_2, implying the two alloyed systems are more destabilized. In fact, some alloying elements considered here can form compounds with Mg and hydrogen, or form complex magnesium hydrides.[27] The influence of alloying elements on the stability of MgH_2 should be addressed by considering the formation of these second phases as discussed below.

TABLE IV. Total energy E^s_{tot}, heat of formation ΔH, and stability parameter $\Delta E'_r$ of $MgCu_2$, TiH_2, Mg_2NiH_4, and Mg_2FeH_6, in comparison with experimental values.

		ΔH (kJ/molH_2)		
	E^s_{tot} (Ry/unit cell)	Present	Expt.	$\Delta E'_r$ (kJ/molH_2)
$MgCu_2$	−7020.797210	−130.79[a]	—	82.18
TiH_2	−1710.076807	−174.68	−164[b]	43.60
Mg_2NiH_4	−3847.687365	−59.35	−62.7[c]	63.17
Mg_2FeH_6	−3354.126006	−124.15	−79.2[b]	67.54

[a]unit: kJ/mol.
[b]Reference 30.
[c]Reference 28.

B. Formation of the second phase and stability of the compounds

As mentioned above, we estimated the influence of the alloying elements on the stability of MgH_2 by assuming that the additions do not form a compound with the host element Mg or H. In fact, some alloying elements, such as Ti, Fe, and Ni, can form compounds with either magnesium (Mg_2FeH_6, Mg_2NiH_4) or hydrogen (TiH_2). In the parallel experiments carried out in our group, it was found that some second phases were formed during ball milling. For example, TiH_2 compound was identified in the MgH_2-Ti system, $MgCu_2$ in the MgH_2-Cu system, and Mg_2NiH_4 in the MgH_2-Ni system.[27] Considering these experimental findings, the influence of compound-forming alloying elements on the stability of MgH_2 was reestimated according to the formation of the second phase as follows:

$$\Delta E'_r = \begin{cases} E_{\text{tot}}(Mg_8Ti_2H_{20}) - 8E_{\text{tot}}(MgH_2) - 2E_{\text{tot}}(TiH_2) & \text{for } MgH_2\text{-Ti}, \\ E_{\text{tot}}(Mg_8Ni_2H_{20}) - 6E_{\text{tot}}(MgH_2) - 2E_{\text{tot}}(Mg_2NiH_4) + 2E_{\text{tot}}(Mg) & \text{for } MgH_2\text{-Ni}, \\ E_{\text{tot}}(Mg_8Fe_2H_{20}) - 4E_{\text{tot}}(MgH_2) - 2E_{\text{tot}}(Mg_2FeH_6) & \text{for } MgH_2\text{-Fe}, \\ E_{\text{tot}}(Mg_8Cu_2H_{20}) - 10E_{\text{tot}}(MgH_2) - E_{\text{tot}}(MgCu_2) & \text{for } MgH_2\text{-Cu}. \end{cases} \quad (4)$$

To estimate the value of $\Delta E'_r$, one needs to calculate the total energy of the second phases involved, and it was calculated with the present code using the experimental lattice parameters, but no geometry optimization was performed for these second phases. The calculated total energies and heat of formation of these compounds are listed in Table IV. Also the experimental values of the heat of formation of these phases are listed in the table for comparison. The calculated heat of formation of these compounds is in good agreement with the experimental values, except for Mg_2FeH_6, the theoretical value of which is about 60% larger than the experimental data. The values of $\Delta E'_r$ also shown in Table IV suggest that the assumed structure for which Mg atoms were replaced by alloying atoms is unstable. The system may decompose to MgH_2 and a second phase through structural relaxation. The dehydriding behavior of the considered systems will then be influenced by the formation of the second phase.

C. Electronic structures

The total and partial densities of states (DOS) of the magnesium hydride are shown in Fig. 3. The total DOS shows five bonding peaks in the energy range between the Fermi level and −6.0 eV. The three main peaks (between −2.0 and

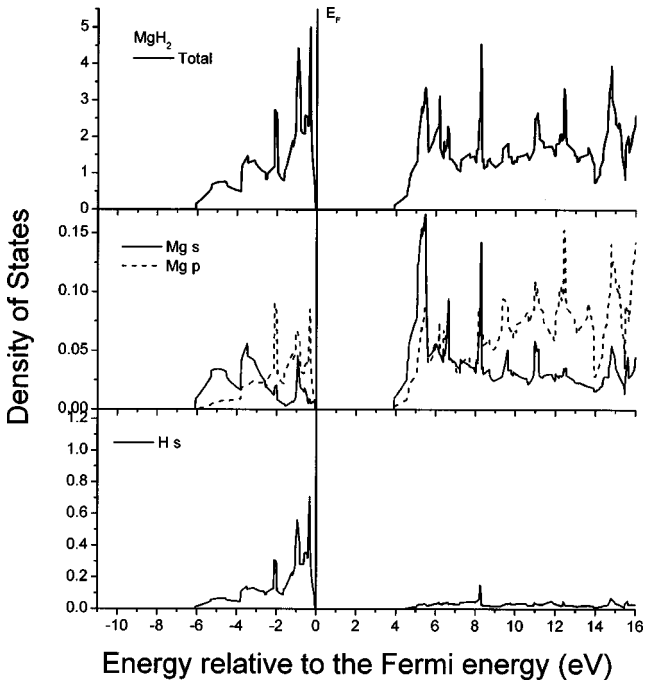

FIG. 3. Total and partial densities of states of the MgH_2 system.

0 eV) are the result of the bonding between H *s* electrons and the Mg *p* and *s* electrons. The other peaks (between −6.0 and −2.5 eV) are caused by the bonding of H *s* and Mg *s* electrons. There is a gap of about 4 eV between the bonding and antibonding states. The total DOS in Fig. 3 shows that the highest bonding band possesses the characteristic of significant *s-p* hybridization, contributed by the hydrogen *s* and magnesium *p* and *s* electrons. This leads to a relatively high formation energy of MgH_2. This aspect was changed in the alloyed $(Mg,X)H_2$ (X=Al, Ti, Fe, Ni, Cu, or Nb) systems.

The alloying elements considered here may be classified into three groups: (I) Ti and Nb, (II) Al and Cu, and (III) Fe and Ni, according to experimental findings.[27–29] In group I, Ti and Nb do not form compounds with Mg, but can form hydrides TiH_2 and NbH_2, respectively. For group II, Al and Cu can form compounds with Mg, but no stable hydrides were found experimentally.[27] The elements Fe and Ni can form hydrides with Mg. These features are determined by the electronic structure.

1. Ti and Nb

Figure 4 shows the total DOSs of the MgH_2-Ti and MgH_2-Nb systems. The common features of the total DOSs of the two systems are that the major bonding peaks near the Fermi energy are mainly controlled by the alloying elements—e.g., Ti or Nb—and the host atoms of magnesium and hydrogen make only a small contribution. In MgH_2-Ti [Fig. 4(a)], the bonding peak near the Fermi energy is contributed by the Ti *d*, the main part, and a weak Mg *s*, and H *s* electrons, implying that the bonding between Ti, Mg, and H is weakened. The *s-p* bonding peaks between magnesium and hydrogen appear in the energy range between −2.5 eV and −5.0 eV in the total DOS. Also there is a weak contribution of the Ti *d* electrons to the bonding peaks. The *s* electron bonding between magnesium and hydrogen appears in the energy region from −5.5 eV to −7.0 eV. For MgH_2-Nb, the partial DOS of magnesium are similar to those for the MgH_2-Ti. The *s-p* bonding between magnesium and hydrogen in MgH_2-Nb is stronger, while the *s-s* bonding between them is weaker than in MgH_2-Ti. The weak bonding between magnesium, hydrogen, and titanium around the Fermi energy may be the reason for the reduced stability of MgH_2 alloyed with elements Ti or Nb.

2. Al and Cu

The total and partial DOSs of MgH_2-Al are shown in Fig. 5(a). There is a weak bonding peak in the total DOS near the Fermi energy, contributed by Al *s* and Mg *s* electrons. The peaks in the total DOS of MgH_2-Al in the energy range between −10.0 eV and −4.0 eV are similar to the total DOS of MgH_2 (Fig. 3). These peaks are the result of the interactions between Al, Mg, and H. The highest peak located at −4.5 eV below the Fermi energy is due to the interaction of Mg2 *p*, Mg3 *p*, H2 *s*, H3 *s*, and Al *p* electrons. The second bonding peak, located at −4.25 eV, is dominated by the Al *s*, Mg *s*, *p*, and H *s* electrons. Considering the fact that the Al atom was surrounded by four H1 and H3 atoms in the supercell used in the present work, the partial DOS of Al, Mg, and H show that the bonding between Al and H3 is the *s-p* interaction, while Al-Mg2 bonding is controlled by the *p-p* and *s-s* interactions. The interaction between Mg and H atoms was weakened by the addition of Al as the partial DOS of both Mg and H atoms near the Fermi energy were significantly reduced.

The total and partial DOS of the MgH_2-Cu are plotted in Fig. 5(b). Four bonding peaks appeared in the total DOS in the energy range from the Fermi energy to −4.0 eV. The peak near the Fermi energy is contributed by Cu *d*, Mg *p*, and H *s* electrons. The contribution of the H2 *s* electron to the peak is smaller than that of the other two H atoms. The highest bonding peak, located at −2.0 eV, shows the characteristics of Cu *d* electrons, while it also contains the contributions of Mg2 *p* and H2 *s* electrons. The other two peaks were dominated by Mg2 *p*, Mg3 *p*, H1 *s*, and H3 *s*, with some level of the Cu *d* electrons.

Comparing the partial DOS of the MgH_2-Cu with that of the MgH_2-Al, we identified that the bonding between Mg and H atoms is stronger in the MgH_2-Cu than that in the MgH_2-Al, due to the presence of a H *s* electron peak near the Fermi energy in the MgH_2-Cu, while in MgH_2-Al system, the peak due to H *s* electron near the Fermi energy can be ignored.

3. Fe and Ni

Figures 6(a) and 6(b) are the total and partial DOS of the MgH_2-Fe and MgH_2-Ni, respectively. In Fig. 6(a), the bonding peaks of the total DOS in the energy range from −1.0 eV to −0.5 eV show an Fe *d* electron characteristic, while Mg2 *p*, Mg3 *p*, and H1 *s* electrons also contributed, to some extent, to the highest bonding peak in the total DOS at about −1.0 eV below the Fermi energy. This feature implies that

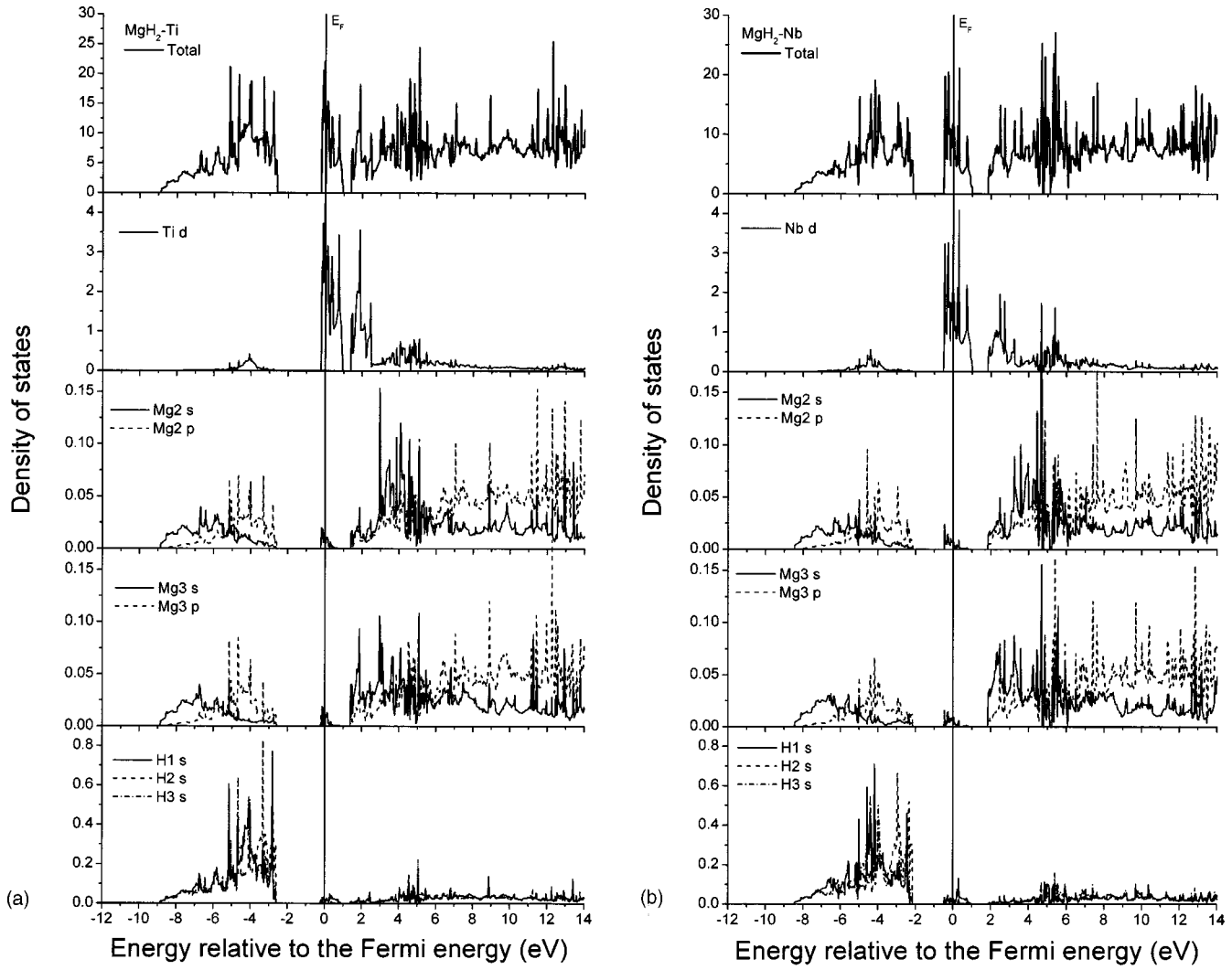

FIG. 4. Total and partial densities of states of the MgH_2-Ti (a) and MgH_2-Nb (b) systems.

there is a relatively weak bonding between Fe, Mg, and H in the MgH_2-Fe system. The other bonding peaks in the total DOS are located in the energy range from -9.0 eV to -2.5 eV below the Fermi energy. These peaks are the result of the interactions between Mg and H. Compared with Fig. 3, the amplitudes of the partial DOS of Mg *p* and H *s* electrons are reduced, implying that the interactions between Mg and H in MgH_2-Fe are weaker than that in MgH_2.

Figure 6(b) shows the total and partial DOS of the MgH_2-Ni. There is a bonding peak near the Fermi energy in the total DOS dominated by the Ni *d*, Mg *s*, and H *s* electrons. Again, the highest peak in the total DOS was dominated by the Ni *d* electrons. In the partial DOS, the magnitude of the Mg *p* electron peaks in the energy range from near -4.0 eV to -2.0 eV below the Fermi energy is reduced in the MgH_2-Ni system compared with that in MgH_2. This leads to a relatively weak interaction between Mg and H atoms. The bonding peak at -4.0 eV in the partial DOS of Mg2 *s*, Mg3 *s* and *p*, H1 *s*, and H3 *s* electrons constitutes the second highest bonding peak in the total DOS. This feature suggests that the interactions between Mg atoms, and between Mg3 and H1 atoms are enhanced as confirmed by the charge distribution on the $(\bar{1}10)$ plane [Fig. 10(b)].

D. Bonding and charge density distribution

In order to understand the microscopic origin of the bonding and the influence of alloying elements on the stability of MgH_2, a charge density analysis was carried out on the $(\bar{1}10)$ plane. Figure 7 shows the charge distribution on the $(\bar{1}10)$ plane of MgH_2. The bonds between Mg and H atoms are clearly seen in the diagram. The influence of alloying elements on the charge density within the $(\bar{1}10)$ plane of the considered systems was analyzed and is presented in Figs. 8–10.

Figure 8 shows the charge distribution of the MgH_2-Ti [Fig. 8(a)] and the MgH_2-Nb [Fig. 8(b)] on the $(\bar{1}10)$, respectively. The Ti-H1 bonds can be identified in Fig. 8(a), while Mg2-H2, and Mg3-H3 bonds are similar to the case of MgH_2, but slightly reduced. The feature of Fig. 8(b), which shows the charge density of MgH_2-Nb on the $(\bar{1}10)$ plane, is

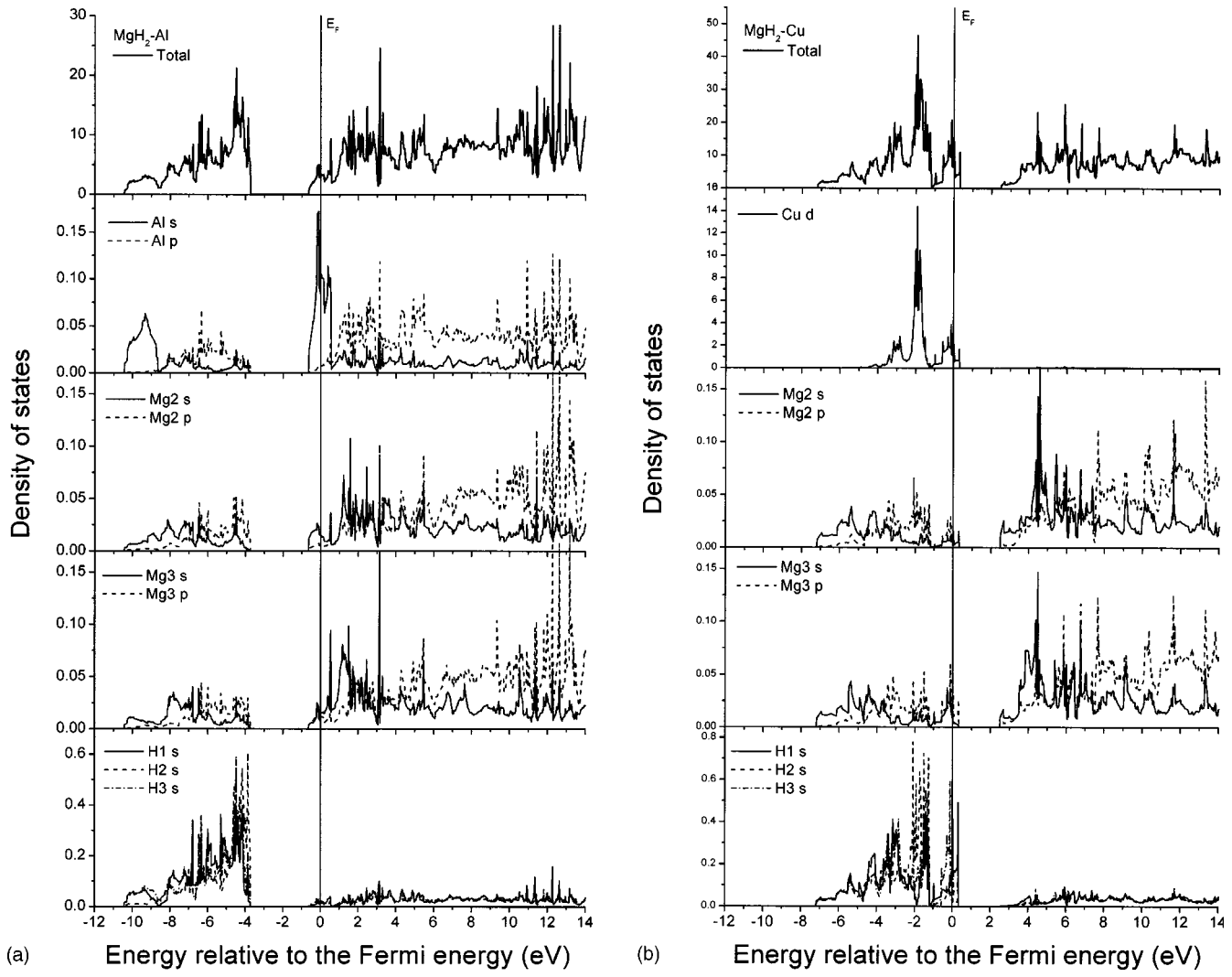

FIG. 5. Total and partial densities of states of the MgH_2-Al (a) and MgH_2-Cu (b) systems.

similar to that of Fig. 8(a). Due to more valence electrons of Nb, a high charge density around the Nb atom was found.

The charge density of MgH_2-Al and MgH_2-Cu on the $(\bar{1}10)$ plane is shown in Figs. 9(a) and 9(b), respectively. In Fig. 9(a), the bonds between Mg2-H1, Mg2-H2, and Mg3-H3 were weakened by the addition of Al atoms, while in Fig. 9(b), the distributions of electrons between Mg and H atoms are similar to that in the MgH_2 system. Only the Mg2-H2 bonds were slightly weakened compared with the case of MgH_2 (Fig. 7).

Figures 10(a) and 10(b) show the charge distributions of the MgH_2-Fe and MgH_2-Ni on the $(\bar{1}10)$ plane, respectively. The bond strength between Mg and H atoms was reduced by the addition of Fe or Ni atoms. This conclusion agrees with the analyses of the DOSs shown in Figs. 6(a) and 6(b).

E. Dehydriding properties

The influence of selected alloying elements on the dehydriding kinetics of MgH_2 was investigated experimentally.[27] It was shown that the dehydriding properties were improved by the addition of the alloying elements. After 10 h, about 2.0 wt% hydrogen was released from the MgH_2-X (X = Cu, Nb, or Ti), 4.0 wt% from the MgH_2-Fe, 5.0 wt% from the MgH_2-Al, and 7.0 wt% from the MgH_2-Ni systems. The dehydrogenation rate is reasonably high in the MgH_2-Al system and most of the 5.0 wt% hydrogen was already released after 4 h.[27] The present first-principles calculations are in agreement with those experimental findings.

For the MgH_2-Ti system, although the stability of MgH_2 was reduced by the addition of titanium, due to the formation of the second phase TiH_2, the hydrogen atoms were held by Ti atoms. However, the DOS [Fig. 4(a)] and the charge distribution on the $(\bar{1}10)$ plane [Fig. 8(a)] of the system show that the bonding strength between Mg and H atoms was slightly reduced, compared with that of MgH_2, and the unit cell volume was also reduced in this system (Table II). The dehydriding properties should then be slightly improved. The alloying element Nb shows a similar effect to Ti due to their similar electronic structural features shown in Figs. 4(b) and 8(b).

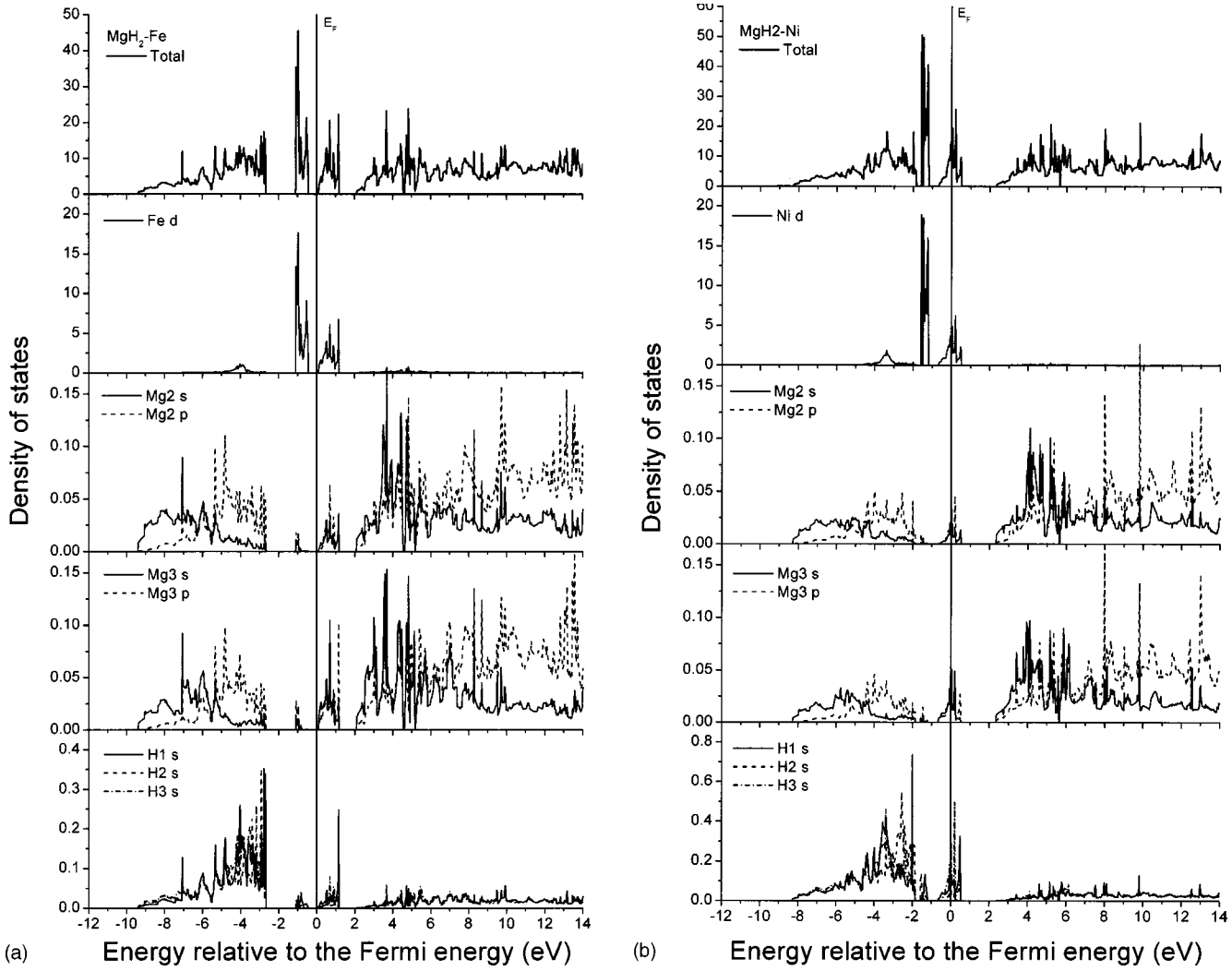

FIG. 6. Total and partial densities of states of the MgH_2-Fe (a) and MgH_2-Ni (b) systems.

For the MgH_2-Al and MgH_2-Fe systems, the stability of the considered system was reduced by 46.22 and 33.35 kJ/mol H_2, respectively. Weak bonding peaks near the Fermi energy were found in the DOS of both MgH_2-Al and MgH_2-Fe systems [Figs. 5(a) and 6(a)]. The charge distributions on the $(\bar{1}10)$ plane [Figs. 9(a) and 10(a)] also show a reduction of the electron density between Mg and H atoms. These electronic structural features support the experimental findings that Al and Fe improve the dehydriding kinetics of MgH_2.[1]

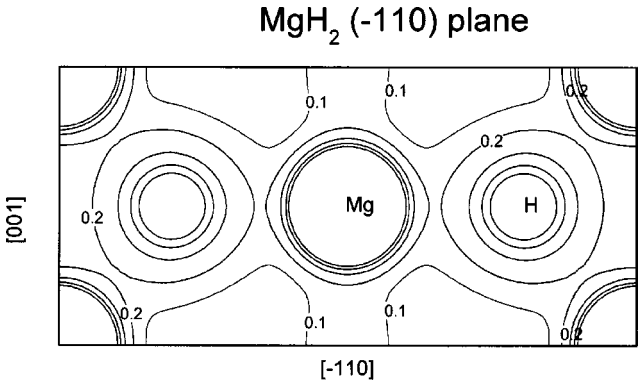

FIG. 7. Charge distribution on the $(\bar{1}10)$ plane of MgH_2. The symmetrically nonequivalent atoms are denoted by 1, 2, and 3.

For the MgH_2-Cu system, the parameter ΔE_r is greater than the absolute value of the heat of formation of MgH_2, implying that the assumed structure is unstable and will most likely decompose to MgH_2 and $MgCu_2$ as found in experiments. On the other hand, nonequilibrium processing, such as mechanical alloying, may embed a certain level of Cu into the MgH_2 compound. The DOS [Fig. 5(b)] show that the bonding peak near the Fermi energy is contributed by Cu *d*, Mg *s*, *p*, and H *s* electrons. It also shows that the bonding between Mg and H2 atoms is weak. This may be due to the formation of $MgCu_2$, in which the Mg atoms were completely held by the Cu atoms, and the previously engaged H atoms were released. Therefore, the H atoms can be readily released from the MgH_2-Cu system, leading to improvement of the dehydriding properties of MgH_2.

For the MgH_2-Ni system, the dehydriding kinetics of MgH_2 was significantly improved by the addition of Ni as mentioned above. The stability parameters ΔE_r and $\Delta E_r'$ are

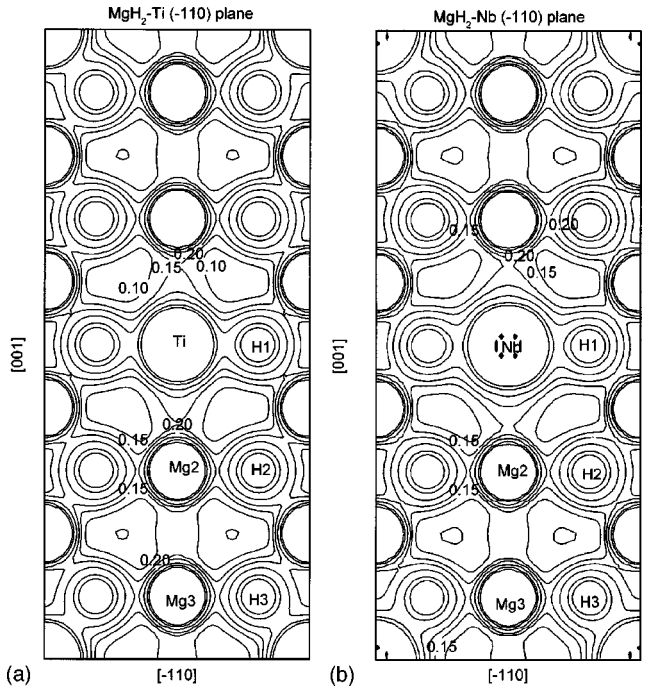

FIG. 8. Charge distribution on the $(\bar{1}10)$ plane of the MgH_2-Ti (a) and MgH_2-Nb (b). The symmetrically nonequivalent atoms are denoted by 1, 2, and 3.

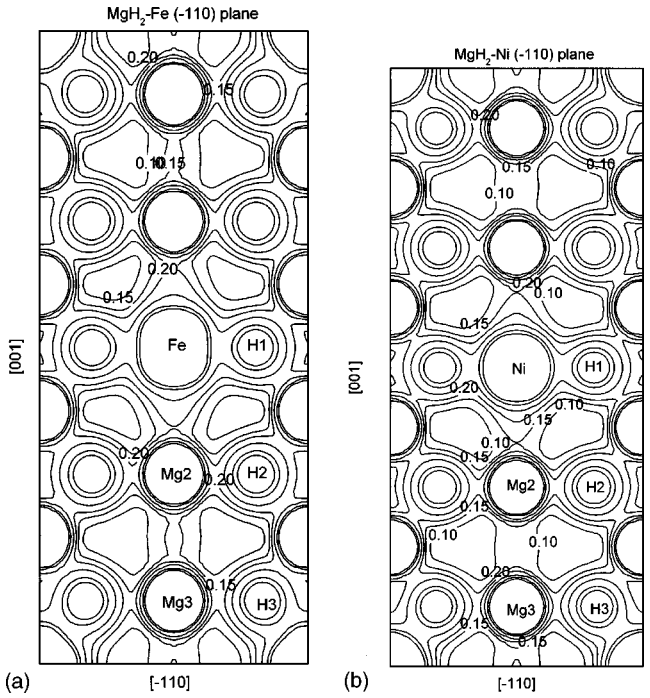

FIG. 10. Charge distribution on the $(\bar{1}10)$ plane of the MgH_2-Fe (a) and MgH_2-Ni (b). The symmetrically nonequivalent atoms are denoted by 1, 2, and 3.

67.88 and 63.17 kJ/mol H_2, respectively, indicating that the assumed structure is more unstable. The DOS [Fig. 6(b)] indicate the possibility of the formation of Mg_2NiH_4 because the main bonding peaks near -1.2 eV below the Fermi energy were contributed by the Ni, Mg, and H atoms. Improvement of the dehydrogenation properties of the system is expected due to the following facts: (i) the bonding between Mg and H was weakened as evidenced by the reduced bonding peaks near the Fermi energy [see the DOS of Fig. 6(b)] and (ii) the formation of the second phase Mg_2NiH_4 with a heat of formation of -62.7 kJ/mol H_2,[28] larger than that of MgH_2. This means that the H atoms in the mixture of MgH_2 and Mg_2NiH_4 compounds can be released more readily than those in MgH_2.

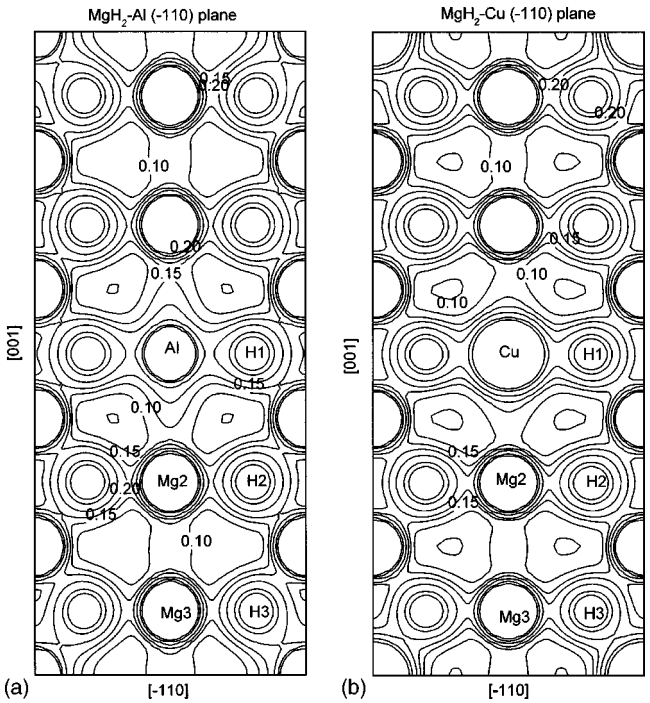

FIG. 9. Charge distribution on the $(\bar{1}10)$ plane of the MgH_2-Al (a) and MgH_2-Cu (b). The symmetrically nonequivalent atoms are denoted by 1, 2, and 3.

IV. CONCLUSIONS

The influence of several alloying atoms X (X = Al, Ti, Fe, Ni, Cu, or Nb) on the stability of the magnesium hydride MgH_2 was clearly demonstrated by means of electronic structure and total energy calculations using the FP-LAPW method within the GGA. The influence of selected alloying elements on the stability of MgH_2 was determined from the difference between the total energy of MgH_2-X and the total energies of the magnesium dihydride, the pure metals, and the hydrogen molecule. Full relaxation of the alloyed systems was considered. The alloying elements mainly influence the position of the matrix atoms in their vicinity: i.e., only the positions of the nearest-neighbor H3 atoms were significantly changed. The influence of alloying elements on the position of the H3 atoms increases in the order of Ti, Nb, Cu, Al, and Ni to Fe. The stability of the alloyed hydride is reduced by the alloying elements, the effectiveness of which decreases from Cu, Ni, Al, Nb, and Fe to Ti. The effect is further enhanced due to the formation of a second phase in the MgH_2-Ti, MgH_2-Ni, MgH_2-Cu, and MgH_2-Fe systems.

Analysis of the DOS and charge distribution shows that the bonding between magnesium and hydrogen was weakened by the additional elements, while there exists stronger bonds between the alloying atom and its nearest-neighbor hydrogen atoms. The interaction is the strongest between the alloying atoms Ti (Nb) and H and the weakest between Al (Cu) and H atoms among the considered elements. The results suggested that the hydriding and dehydriding properties of the magnesium hydride—e.g., dehydriding temperature and/or kinetics—should be improved by the solution of the alloying elements into the compound.

ACKNOWLEDGMENTS

This work was mainly supported by the EPSRC of the United Kingdom (Grant No. GR/R82074/01) and partly supported by the MoST of China (Grant No. TG2000067105).

*Corresponding author. Electronic address: y.song@qmul.ac.uk

[1] X. Shang, M. Bououdina, and Z. X. Guo, J. Alloys Compd. **349**, 217 (2003).
[2] D. L. Douglass, in *Proceedings of the 9th International Symposium on Hydrides for Energy Storage 9*, edited by A. F. Anderson and A. J. Maeland (Pergamon, Oxford, 1978), p. 151.
[3] P. Selvam, B. Viswanathan, C. S. Swamy, and V. Srinivasan, Int. J. Hydrogen Energy **11**, 169 (1986).
[4] N. Gerard and S. Ono, in *Hydrogen in Intermetallic Compounds II, Topics in Applied Physics*, Vol. 64, edited by L. Schlapbach (Springer-Verlag, Berlin, 1992), p. 178.
[5] J. M. Boulet and N. Gerard, J. Less-Common Met. **89**, 151 (1991).
[6] G. Liang, J. Huot, S. Boily, A. Van Neste, and R. Schulz, J. Alloys Compd. **292**, 247 (1999).
[7] P. Selvam, J. Less-Common Met. **163**, 89 (1990).
[8] P. C. Bouten and A. R. Miedema, J. Less-Common Met. **71**, 147 (1980).
[9] D. G. Westlake, J. Less-Common Met. **91**, 1 (1983).
[10] C. D. Gelatt, H. Ehrenreich, and J. A. Weiss, Phys. Rev. B **17**, 1940 (1978).
[11] R. Griessen and A. Driessen, Phys. Rev. B **30**, 4372 (1984).
[12] A. R. Miedema, J. Less-Common Met. **32**, 117 (1973).
[13] R. Griessen and T. Riesterer, in *Hydrogen in Intermetallic Compounds I, Topics in Applied Physics*, Vol. 63, edited by L. Schlapbach (Springer-Verlag, Berlin, 1988), p. 219.
[14] H. Nakamura, D. Nguyen-Manh, and D. G. Pettifor, J. Alloys Compd. **281**, 81 (1998).
[15] H. Yukawa, M. Morinaga, and Y. Takahashi, J. Alloys Compd. **253-254**, 322 (1997).
[16] T. Suenobu, I. Tanaka, H. Adachi, and G. Adachi, J. Alloys Compd. **221**, 200 (1995).
[17] G. N. Garcia, J. P. Abriata, and J. O. Sofo, Phys. Rev. B **59**, 11 746 (1999).
[18] E. Orgaz and M. Gupta, J. Phys.: Condens. Matter **5**, 6697 (1993).
[19] T. Nambu, H. Ezaki, H. Yukawa, and M. Morinaga, J. Alloys Compd. **293-295**, 213 (1999).
[20] W. Wolf and P. Herzig, J. Phys.: Condens. Matter **12**, 4535 (2000).
[21] P. Blaha, K. Schwarz, and J. Luitz, computer code WIEN2K, Vienna University of Technology, 2000.
[22] D. Singh, *Plane Waves, Pseudopotentials, and the LAPW Methods* (Kluwer Academic, New York, 1994).
[23] J. P. Perdew, S. Burke, and M. Ernzerhof, Phys. Rev. Lett. **77**, 3865 (1996).
[24] M. Weinert, E. Wimmer, and A. J. Freeman, Phys. Rev. B **26**, 4571 (1982).
[25] M. Bortz, B. Bertheville, G. Böttger, and K. Yvon, J. Alloys Compd. **287**, L4 (1999).
[26] M. Yamaguchi and E. Akiba, in *Electronic and Magnetic Properties of Metals and Ceramics Part II, Materials Science and Technology*, Vol. 3B, edited by R. W. Cahn, P. Haasen, and E. J. Kramer (VCH, Weinheim, 1994), p. 333.
[27] C. X. Shang, M. Bouodina, Y. Song, and Z. X. Guo, Mater. Sci. Eng. A (to be published).
[28] M. Yamaguchi and E. Akiba, in *Electronic and Magnetic Properties of Metals and Ceramics Part II, Materials Science and Technology*, Vol. 3B, edited by R. W. Cahn, P. Haasen, and E. J. Kramer (VCH, Weinheim, 1994), p. 333.
[29] See for example, *Hydrogen in Intermetallic Compounds I, Topics in Applied Physics*, Vol. 63, edited by L. Schlapbach (Springer-Verlag, Berlin, 1988).
[30] http://hydpark.ca.sandia.gov